TISSUE ENGINEERING: Part A
Volume 27, Numbers 1 and 2, 2021

DOI: 10.1089/ten.tea.2020.0103

termis
Tissue Engineering
& Regenerative Medicine
International Society

ORIGINAL ARTICLE

Combined Hydrogel and Mesenchymal Stem Cell Therapy for Moderate-Severity Disc Degeneration in Goats

Chenghao Zhang, PhD,[1–3] Sarah E. Gullbrand, PhD,[1,3] Thomas P. Schaer, VMD,[4] Sophie Boorman, VMD,[4] Dawn M. Elliott, PhD,[5] Weiliam Chen, PhD,[6] George R. Dodge, PhD,[1,3] Robert L. Mauck, PhD,[1,3] Neil R. Malhotra, MD,[1,2] and Lachlan J. Smith, PhD[1–3]

Intervertebral disc degeneration is a cascade of cellular, structural, and biomechanical changes that is strongly implicated as a cause of low-back pain. Current treatment strategies have poor long-term efficacy as they seek only to alleviate symptoms without preserving or restoring native tissue structure and function. The objective of this study was to evaluate the efficacy of a combined triple interpenetrating network hydrogel (comprising dextran, chitosan, and teleostean) and mesenchymal stem cell (MSC) therapy targeting moderate-severity disc degeneration in a clinically relevant goat model. Degeneration was induced in lumbar discs of 10 large frame goats by injection of chondroitinase ABC. After 12 weeks, degenerate discs were treated by injection of either hydrogel alone or hydrogel seeded with allogeneic, bone marrow-derived MSCs. Untreated healthy and degenerate discs served as controls, and animals were euthanized 2 weeks after treatment. Discs exhibited a significant loss of disc height 12 weeks after degeneration was induced. Two weeks after treatment, discs that received the combined hydrogel and MSC injection exhibited a significant, 10% improvement in disc height index, as well as improvements in histological condition. Discs that were treated with hydrogel alone exhibited reduced tumor necrosis factor-α expression in the nucleus pulposus (NP). Microcomputed tomography imaging revealed that the hydrogel remained localized to the central NP region of all treated discs after 2 weeks of unrestricted activity. These encouraging findings motivate further, longer term studies of therapeutic efficacy of hydrogel and MSC injections in this large animal model.

Keywords: nucleus pulposus, preclinical, caprine, spine, intervertebral disc, therapy

Impact Statement

Low-back pain is the leading cause of disability worldwide, and degeneration of the intervertebral discs is considered to be one of the most common reasons for low-back pain. Current treatment strategies focus solely on alleviation of symptoms, and there is a critical need for new treatments that also restore disc structure and function. In this study, using a clinically relevant goat model of moderate-severity disc degeneration, we demonstrate that a combined interpenetrating network hydrogel and mesenchymal stem cell therapy provides acute improvements in disc height, histological condition, and local inflammation.

Introduction

Low-back pain is the leading cause of disability worldwide.[1,2] Degeneration of the intervertebral discs is a cascade of cellular, structural, and biomechanical changes closely linked to aging, and is considered to be one of the most common reasons for low-back pain.[3,4] Current treatment strategies for disc degeneration, be they conservative or surgical, have poor long-term efficacy as they seek only to alleviate symptoms without preserving or restoring native tissue structure and mechanical function.

[1]Translational Musculoskeletal Research Center, Corporal Michael J. Crescenz Philadelphia VA Medical Center, Philadelphia, Pennsylvania, USA.
Departments of [2]Neurosurgery and [3]Orthopaedic Surgery, Perelman School of Medicine, University of Pennsylvania, Philadelphia, Pennsylvania, USA.
[4]Comparative Orthopaedic Research Laboratory, New Bolton Center, School of Veterinary Medicine, University of Pennsylvania, Kennett Square, Pennsylvania, USA.
[5]Department of Biomedical Engineering, University of Delaware, Newark, Delaware, USA.
[6]Department of Surgery, New York University School of Medicine, New York, New York, USA.

Of the ~15 million low-back pain patients who present to physicians each year in the United States, around 4 million will have a diagnosis of moderate-severity degeneration, be unresponsive to conservative treatments such as physical therapy and steroid injections, and not be considered good candidates for surgical intervention such as spinal fusion.[5] There is an overwhelming clinical need for improved treatment options for these patients.

Each intervertebral disc comprises three main substructures: a central, gelatinous and highly hydrated nucleus pulposus (NP); a peripheral, fibrocartilaginous annulus fibrosus (AF); and superiorly and inferiorly, two hyaline cartilage endplates that interface with the vertebral bodies.[6] The earliest signs of disc degeneration typically manifest first in the NP, where persistent, local inflammation drives proteoglycan loss.[4,7,8] The resulting decrease in hydrostatic pressure compromises the ability of this tissue to transfer and distribute compressive loads, which leads to progressive deterioration of the entire intervertebral joint. For this reason, there is keen interest in developing therapeutic approaches that preserve or regenerate NP tissue and prevent progression of the degenerative cascade.[9]

To this end, both stem cells and injectable hydrogel implants are currently being investigated as potential NP therapies.[10,11] Stem cells have the potential to ameliorate disc inflammation and prevent progression of degeneration, while simultaneously potentiating reconstitution of native tissue. Mesenchymal stem cells (MSCs), specifically, hold significant promise due to their relative ease of isolation, safety profile, and ability to adopt phenotypes similar to native NP cells.[12–14] Injectable hydrogels can provide acute structural and mechanical support to the degenerate disc, while also acting as a delivery vehicle for MSCs and other bioactive factors.[10,15]

Our group has developed and characterized a triple interpenetrating network hydrogel comprising three naturally derived materials: *N*-carboxyethyl chitosan, oxidized dextran, and teleostean. When solutions of these three components are combined, they rapidly form a stable hydrogel by Schiff base formation between the –CHO on the oxidized dextran and the $-NH_2$ on the teleostean and chitosan.[16,17] Through a series of *ex vivo* studies, we established the suitability of this hydrogel as an NP implant material.[18–20] Specifically, we demonstrated that it is suitable for minimally invasive delivery to the disc NP where it undergoes rapid *in situ* gelation, mimics the bulk mechanical properties of and interdigitates with native NP tissue, remains completely contained within the disc after 10,000 loading cycles,[19] and can restore the stiffness and range of motion of degenerate discs.[18] Furthermore, we showed that this hydrogel can act as a delivery vehicle for MSCs, supporting both viability and extracellular matrix production.[20] Most recently, we demonstrated the translational feasibility of this hydrogel in a goat model of disc degeneration.[18] This goat model recapitulates key features of moderate-severity human disc degeneration, including clinically relevant structural, compositional, biomechanical, and inflammatory changes.[21,22] Through incorporation of zirconia nanoparticles into the hydrogel, we were able to confer radiopacity, thus enabling noninvasive assessment of retention and distribution following *in vivo* delivery.[18]

The objective of this study was to build on this previous work by investigating the efficacy of combined hydrogel and MSC injections for treating moderate-severity intervertebral disc degeneration in a goat model. Specifically, we investigated the potential for this therapy to improve disc height, condition, and inflammation 2 weeks after delivery. An additional objective was to confirm the *in vivo* retention and distribution of both the injected hydrogel and MSCs within the disc NP at this early time point.

Methods

Animals and study design

This study was approved by the Institutional Animal Care and Use Committee of the University of Pennsylvania and the Animal Ethics Subcommittee of the Corporal Michael J. Crescenz Philadelphia VA Medical Center. All animal studies were performed in compliance with the National Institutes of Health Guide for Care and Use of Laboratory Animals and the ARRIVE guidelines.[23] Ten, skeletally mature, large frame castrated male goats (Thomas D. Morris, Inc., Reisterstown, MD), ranging between 2 and 4 years of age, were used in this study. Male goats were used exclusively to maximize disc size, although this precluded an assessment of sex-dependent effects on treatment efficacy. Following an acclimatization phase, animals underwent two surgical procedures 12 weeks apart (Fig. 1). The first surgery was performed to induce moderate-severity disc degeneration in four lumbar levels (L1–L5) by intradiscal injection of chondroitinase ABC (ChABC) as described previously,[18,21] while a second surgery was performed 12 weeks later to deliver therapies. Animals were housed in a 25×25 m outdoor barn in groups of two or three with access to full exercise, and evaluated daily by a veterinarian for signs of pain, neurologic deficits, behavior changes, or gait abnormalities for the duration of the study. Animal diet consisted of grass hay provided *ad libitum*, plus up to 1 lb of goat chow per day calculated based on body score. Experimental outcomes included disc height index (DHI) measured from plain radiographs, disc condition measured using *ex vivo* magnetic resonance imaging (MRI), semiquantitative histological grading, and disc inflammation assessed by measuring tumor necrosis factor (TNF)-α immunopositive cells in the NP and AF. In addition, three-dimensional (3D) *ex vivo* assessment of hydrogel distribution was assessed using microcomputed tomography (microCT), and distribution of injected MSCs was assessed immunohistochemically.

Surgical procedure to induce degeneration

An initial surgical procedure was performed to induce disc degeneration as described previously.[18,21] Animals were anesthetized by intravenous injection of ketamine (11–33 mg/kg) and midazolam (0.5–1.5 mg/kg), endotracheal intubation, and maintained on an isoflurane-oxygen mixture for the duration of the surgical procedure. Using an open, left lateral, retroperitoneal transpsoatic approach, the lumbar spine was exposed and L1–2, L2–3, L3–4, and L4–5 discs received an injection of ChABC (1 U suspended in 200 μL of sterile saline) into the NP under fluoroscopic guidance using a 22-gauge stainless steel Quincke spinal needle (Popper and Sons, Inc., New Hyde Park, NY) attached to a

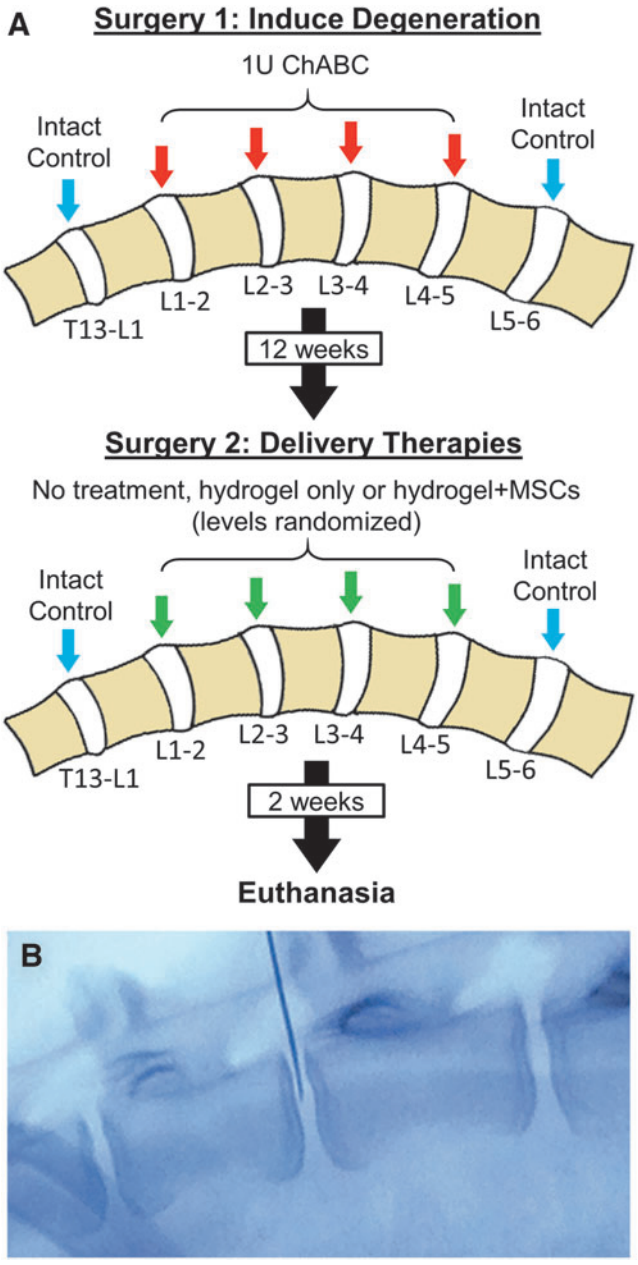

FIG. 1. **(A)** Study design. **(B)** Intraoperative fluoroscopy showing delivery of therapeutic agents to the disc NP using a 22-gauge spinal needle. NP, nucleus pulposus. Color images are available online.

250 μL glass syringe (Hamilton Company, Inc., Reno, NV). The T13–L1 or L5–6 discs served as intact, healthy controls. The incision was closed in layers, and the animal hand-recovered and returned to their presurgery housing with unrestricted activity. Animals were administered perioperative transdermal fentanyl (2.5 mcg/kg/h) and intravenous flunixin meglumine (Banamine, 1.1 mg/kg) for analgesia. Florfenicol (40 mg/kg) was administered for perioperative antimicrobial prophylaxis lasting for 24 h.

Hydrogel and MSC preparation

MSCs were obtained from the bone marrow of three study animals during the first surgery to induce disc degeneration described above. Briefly, following standard aseptic technique, an 11-gauge, 101 mm T-handle Jamshidi™ bone marrow biopsy needle with a trocar-tapered stylet point and a triple-crown cannula tip was used to aspirate bone marrow (1–2 mL) from the iliac crest into a 10 mL heparinized syringe (20 U heparin/1 mL fresh bone marrow) and immediately stored on ice. Following the procedure, a sterile dressing was applied. Marrow was plated in basal media (Dulbecco's modified Eagle medium with 10% fetal bovine serum and 1% penicillin/streptomycin/fungizone), and MSCs were obtained by plastic adherence and expanded through 1–2 additional passages in basal media in normoxia before being cryopreserved until required for treatments. Allogeneic cells were used for all treatments (i.e., recipient and donor animals were not the same). Approximately 2 weeks before the second surgery described below, MSCs were thawed and expanded to confluence through one additional passage, and transfected with green fluorescent protein (GFP) to facilitate postmortem identification using immunohistochemistry. To fabricate the hydrogel, oxidized dextran and *N*-carboxyethyl chitosan (Endomedix, Inc., Montclaire, NJ) were synthesized as described previously.[16] Aqueous solutions of 20% teleostean (Sigma Aldrich, St. Louis, MO), 3% *N*-carboxyethyl chitosan, and 7.5% oxidized dextran were mixed at a ratio of 1:1:2. MSCs were suspended in the 7.5% oxidized dextran such that a seeding density of 10 million cells/mL of hydrogel was achieved after mixing the three components. For a subset of treated discs ($n = 13$), the hydrogel was rendered radiopaque by the inclusion of zirconia nanoparticles, as described previously,[18] to enable intraoperative visualization through fluoroscopy and *ex vivo* visualization through microCT. Zirconia nanoparticles (30 wt%; Sigma Aldrich) were added to the aqueous teleostean before mixing of the three hydrogel components. Hydrogel components were sterilized before delivery by exposure to ultraviolet light.

Surgical procedure to deliver therapies

Twelve weeks following the initial surgery to induce degeneration, a second surgery was performed to deliver therapies. Each degenerate disc was randomly assigned to one of three groups: (1) treatment with hydrogel alone; (2) treatment with combined hydrogel + MSCs; or (3) untreated degenerate controls (Fig. 1). Nondegenerate T13–L1 or L5–6 discs were maintained as intact, healthy controls. Using similar surgical preparation, anatomic approach, and anesthesia to the first surgery, discs were exposed, and therapies injected using a 22-gauge spinal needle attached to a 250 μL syringe under fluoroscopic guidance. MSCs were suspended in the hydrogel as described above immediately before injection. The injection volume was 0.55 ± 0.27 mL (using tactile feedback, the maximum injectable volume until ejection was observed refluxing into the needle track), and was not significantly different between treatment groups. Animals were hand-recovered from surgery as described above and returned to their presurgery housing with unrestricted activity. Two weeks following this second surgery, animals were euthanized by an overdose of sodium pentobarbital solution in accordance with American Veterinary Medical Association guidelines, and lumbar spines harvested for *ex vivo* analyses.

Radiographic assessment of disc height

To assess changes in disc height with degeneration and following treatment, lateral plain radiographs of the lumbar spine were obtained *in vivo* in a standing and fully weight-bearing position immediately before each surgery (i.e., 0 and 12 weeks, preoperatively), and then again at 14 weeks (2 weeks following the second surgery to delivery therapies). DHI (disc height normalized to adjacent vertebral body length) was quantified by two blinded assessors using a custom MATLAB program (Mathworks, Natick) as described previously.[24]

Magnetic resonance imaging

Following euthanasia, lumbar spines were harvested and imaged using MRI to assess disc condition. Specifically, discs were imaged using a 3 T clinical MRI scanner (Siemens Magnetom TrioTim, Munich, Germany) with a voxel size of 0.6 mm × 0.6 mm × 5 mm. T2-weighted mid-sagittal images were obtained for semiquantitative Pfirrmann grading as previously described.[21] Following MRI, posterior bony elements were removed, and spines were divided into vertebra-disc-vertebra segments for further analysis.

Microcomputed tomography

Spine segments that received an injection of zirconia nanoparticle-labeled hydrogel ($n = 13$) were imaged using microCT at an isotropic resolution of 20.5 μm to visualize the 3D distribution of radiopaque hydrogel within the disc space (μCT 50; Scanco, Brüttisellen, Switzerland). A volume of interest constituting the entirety of the disc space was generated by manual segmentation, and the hydrogel was manually thresholded and analyzed using the Scanco software. A composite heat map showing relative, regional localization of hydrogel across all discs was generated using ZEN lite 2.5 (Carl Zeiss Microscopy GmbH, Jena, Germany).

Histological grading

Following microCT imaging, all spine segments were fixed in buffered 10% formalin, decalcified in formic and ethylenediaminetetraacetic acids (Formical 2000; StatLab, McKinney), and processed into paraffin. Mid-sagittal 10 μm sections were cut and double stained with either Alcian Blue and Picrosirius Red for glycosaminoglycan and collagen distribution, respectively, or hematoxylin and eosin to demonstrate cellularity. Disc condition was assessed using semiquantitative histological grading as previously described.[21] For each disc, two randomly selected images were obtained at 4× and 20× magnification for each of the AF, NP, and cartilaginous end plates, with care taken to avoid regions containing injected hydrogel that could confound grading. Semiquantitative grading was performed by three blinded assessors (averaged) using a modification of the scheme proposed by Masuda *et al.*[25] Grading criteria included AF organization, AF/NP border, cartilaginous end plate structure, NP matrix, and NP cellularity, which was each assigned a score from 0 (completely healthy) to 100 (severely degenerated). Overall histological grade was calculated as the sum of all five subcriteria.

Immunohistochemistry

To assess the effects of therapies on local disc inflammation, TNF-α expression was measured in the NP and AF using immunohistochemistry as described previously.[22] Antigen retrieval was carried out on rehydrated sections enzymatically using proteinase K (10 mg/mL; Roche Diagnostics, Basel, Switzerland) for 4 min at 37°C. Sections were treated with 3% hydrogen peroxide for 12 min to block endogenous peroxidase activity, followed by Background Buster (Innovex Biosciences, Richmond) for 10 min at room temperature to block nonspecific protein binding. Sections were then incubated with an anti-TNF-α antibody (ab6671, 1:200 dilution; Abcam Plc, Cambridge) overnight at 4°C. Antibody staining was visualized using the Vectastain Elite ABC-Peroxidase Kit (Vector Laboratories, Burlingame) and diaminobenzidine chromogen (Thermofisher Scientific, Waltham) according to the manufacturer's protocol. Finally, sections were counterstained with hematoxylin QS (Vector Laboratories) and cover slipped with an aqueous mounting medium (Agilent, Santa Clara). For analysis, all slides were imaged under bright field light microscopy (Eclipse 90i; Nikon, Tokyo, Japan). Three randomly selected regions of interest within both the NP and AF were analyzed. For each region, the number of immunopositive cells was counted and normalized as a percentage of the total number of cells present. Cell counting for each region was performed by three individuals who were blinded to the study groups and averaged. The average result for all three regions (in the NP or AF) was then determined and taken as a single biological replicate for statistical comparisons. Localization of injected GFP-labeled MSCs was assessed immunohistochemically using an anti-GFP antibody (ab290, 1:200 dilution; Abcam). Antigen retrieval, blocking, incubation, and staining steps were identical to those described above. Sections were imaged under bright field microscopy, and the presence of GFP-positive MSCs within the hydrogel was qualitatively assessed.

Statistical analyses

Statistical analyses were conducted using SYSTAT 19 (Systat Software, Inc., San Jose, CA). Normality of each data set was assessed using Shapiro-Wilk tests. Changes in disc height over time (0 vs. 12 vs. 14 weeks) for each study group were evaluated using repeated-measures analysis of variance followed by *posthoc* Tukey's tests, with data presented as mean ± standard deviation. Differences in MRI Pfirrmann grade, histology grade, and TNF-α expression between study groups were established using one-way Kruskal-Wallis tests followed by pairwise, *posthoc* Dunn's tests, with data presented as median and interquartile range. Statistical significance was defined as $p < 0.05$.

Results

All 10 animals recovered from surgical procedures without adverse events. One animal developed cyclic episodes of pyrexia, dullness, and inappetence, and was euthanized before reaching the designated endpoint. Postmortem and histopathology revealed an aseptic fibrinous peritonitis. For a small number of discs ($n = 5$), imaging and histology revealed large end plate disruptions. These disruptions were present in at least one disc for all

study groups, except healthy controls (Supplementary Fig. S1). These discs were excluded from analyses, leaving the following sample sizes for each study group: healthy controls: $n=10$; untreated degenerated controls: $n=5$; hydrogel alone: $n=10$; and combined hydrogel and MSCs: $n=9$. In addition, for disc height measurements, as intact control discs (T13–L1 and L5–6) were located at the outer margins of the radiographs, parallax error prevented accurate repeated disc height measurements for these discs in all but four animals.

Hydrogel distribution

Three-dimensional reconstructions and axial composite projections of all zirconia-labeled injected discs (Fig. 2) showed that delivered hydrogel was predominantly located in the central NP region, although some hydrogel was also evident distributed throughout the lamellar structure of the AF.

Disc height

For all study groups that received an injection of ChABC, DHI after 12 weeks (immediately before delivery of therapies) was significantly decreased (degenerate control: $63.88\pm11.46\%$ vs. 0 weeks; hydrogel alone: $67.76\pm10.42\%$ vs. 0 weeks; and hydrogel + MSCs: $65.20\pm15.69\%$ vs. 0 weeks, $p<0.005$ for all). At 14 weeks (2 weeks following delivery of therapies), discs treated with hydrogel + MSCs exhibited a significant, 10% improvement in DHI ($75.06\pm16.53\%$ of 0 weeks, $p=0.005$ vs. both 12 and 0 weeks). For discs treated with hydrogel alone, DHI improved (5%), but not significantly compared to 12 weeks ($72.72\pm13.34\%$ vs. 0 weeks, $p<0.005$ and $p=0.278$ vs. 0 and 12 weeks, respectively). Of discs treated with hydrogel alone, 5 out of 10 (Fig. 3D) exhibited an improvement in DHI 2 weeks after treatment, while of those discs treated with hydrogel + MSCs, 8 out of 9 discs (Fig. 3E) exhibited improved DHI. For untreated, degenerate control discs, DHI declined slightly from 12 to 14 weeks ($62.04\pm9.84\%$ vs. 0 weeks, $p<0.005$ and $p=0.417$ vs. 0 and 12 weeks, respectively). For healthy controls, DHI did not change significantly across the study duration.

Magnetic resonance imaging

Semiquantitative Pfirrmann grading from T2-weighted, mid-sagittal MRI images of *ex vivo* lumbar spines was used to assess disc condition (Fig. 4). For degenerate control discs, Pfirrmann grades were significantly worse compared to healthy control discs ($p=0.007$). For discs treated with either hydrogel alone or hydrogel + MSCs, Pfirrmann grades were significantly worse than healthy controls ($p<0.005$ for both), and not significantly improved compared to untreated degenerate control discs.

Histological grading

Alcian blue-picrosirius red staining showed clear differences in disc condition with degeneration and treatment (Fig. 5A), although variability was evident within each study group. Hydrogel could be easily identified in the NPs of treated discs both morphologically and due to intense picrosirius red staining (Fig. 5A, arrows). Semiquantitative histological grading was used to examine improvements in disc condition following treatment (Fig. 5B–G). Five grading parameters were examined, which were also summed to determine overall grade. NP cellularity, NP extracellular matrix, and AF/NP border were each significantly worse for both untreated degenerate controls ($p<0.005$, $p=0.017$, and $p<0.005$, respectively) and discs treated with hydrogel alone ($p=0.047$, $p=0.017$, and $p=0.012$, respectively); however, for discs treated with combined hydrogel + MSCs, these parameters were improved, and not significantly different from healthy control discs. AF organization was significantly worse than healthy controls for untreated degenerate control discs ($p=0.012$), but for discs treated with either hydrogel alone, or hydrogel + MSCs, it was not significantly different from healthy control discs. End plate structure was significantly worse for hydrogel alone-treated discs ($p<0.005$), but for degenerate controls and discs treated with combined hydrogel + MSCs, it was not significantly different from healthy control discs. Finally, overall histological grade was significantly worse for both untreated degenerate controls and discs treated with hydrogel alone ($p=0.007$ and $p=0.012$, respectively); however, for discs treated with combined hydrogel + MSCs, overall grade was improved, and not significantly different from healthy controls.

TNF-α expression levels

In our prior study, we demonstrated that disc degeneration in this goat model is characterized by elevated expression of physiologically relevant cytokines, including

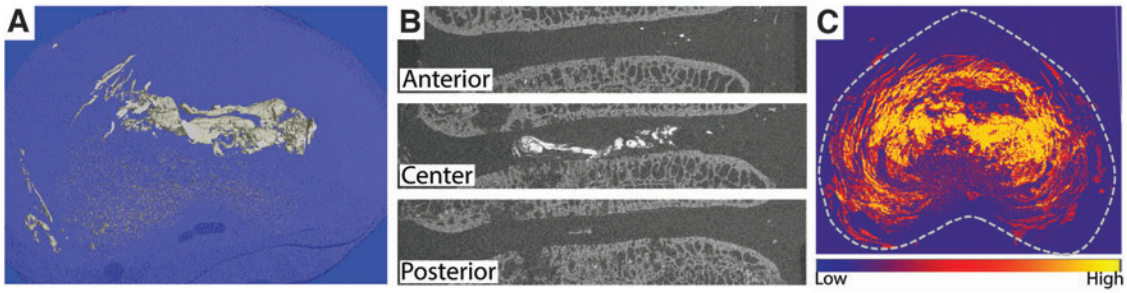

FIG. 2. Visualization of zirconia-labeled hydrogel distribution in intervertebral discs 2 weeks after *in vivo* delivery. **(A)** Three-dimensional reconstruction of hydrogel in a single disc. **(B)** Corresponding coronal slices; and **(C)** composite axial intensity projection for 13 discs illustrating hydrogel predominantly located in the central, NP region. Higher intensity indicates more frequent location of hydrogel. Color images are available online.

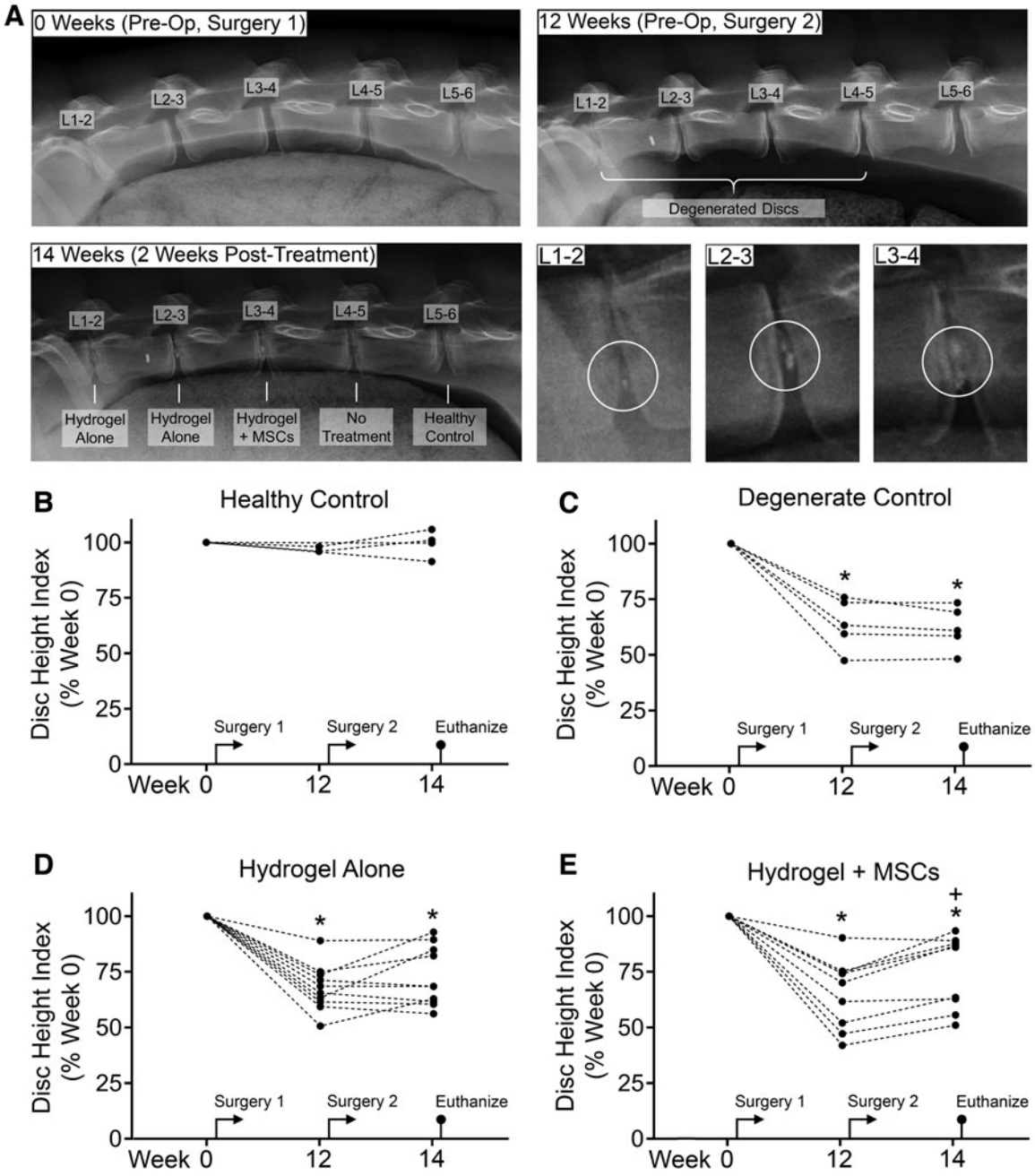

FIG. 3. **(A)** Representative lateral radiographs of goat lumbar spines at 0 weeks (immediately before Surgery 1 to induce degeneration using chondroitinase ABC), 12 weeks (immediately before Surgery 2 to delivery therapies), and 14 weeks (2 weeks after delivery of therapies and immediately before euthanasia). Higher magnification images show hydrogel (*circled*) in treated discs at 14 weeks. **(B–E)** Disc height index for each study group at 0, 12, and 14 weeks, expressed as a percentage of week 0. $^{*}p<0.05$ versus week 0; $^{+}p<0.05$ versus week 12; repeated-measures analysis of variance with *posthoc* Tukey's tests.

TNF-α. In this study, we examined TNF-α expression levels (as the percentage of immunopositive cells) in the NP and AF in response to treatment (Fig. 6). As expected, for untreated degenerate control discs, TNF-α expression was significantly elevated in both the NP and AF compared to healthy controls ($p<0.005$ for both). For discs treated with hydrogel alone, TNF-α expression in the NP was reduced and not significantly different from healthy control discs, but still significantly elevated in the AF ($p=0.046$). For discs treated with combined hydrogel + MSCs, TNF-α expression remained significantly elevated compared to healthy controls in both the NP ($p=0.007$) and AF ($p=0.006$).

Regional localization of injected MSCs

Immunohistochemical staining for GFP was used to successfully confirm the retention of MSCs within the hydrogel of treated discs (Fig. 7). For discs that received the

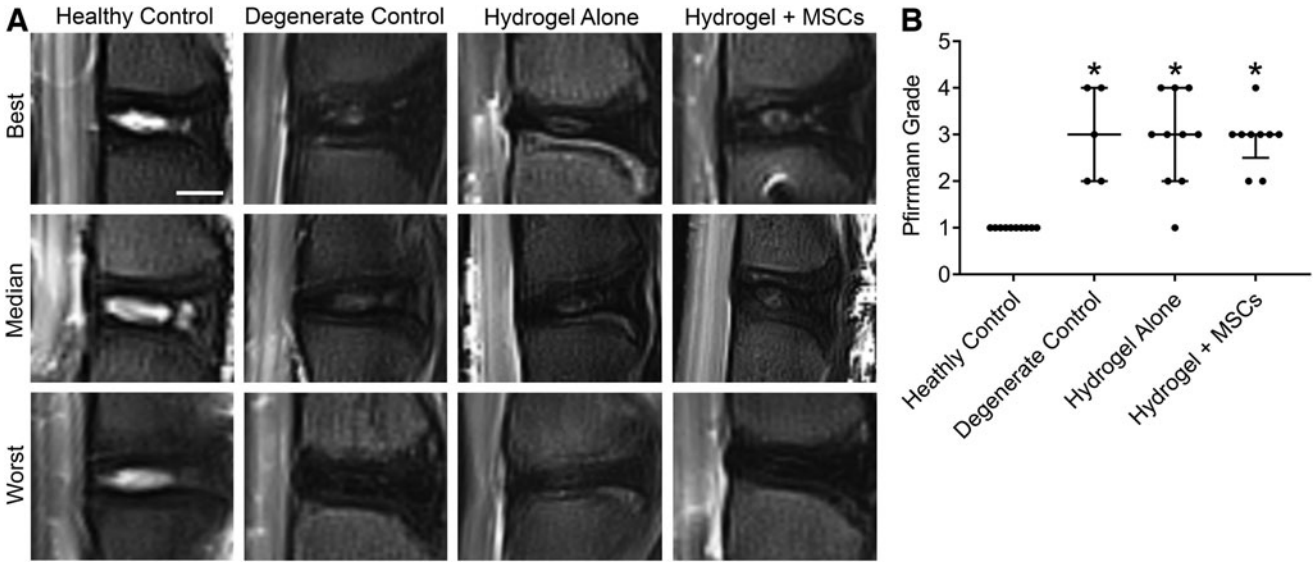

FIG. 4. **(A)** Representative T2-weighted, mid-sagittal magnetic resonance imaging illustrating best, median, and worst discs from each study group. **(B)** Semiquantitative Pfirrmann grades. $*p < 0.05$ versus healthy control; Kruskal-Wallis tests with *posthoc* Dunn's tests; data presented as median and interquartile range.

combined treatment, no GFP-labeled MSCs were observed outside discs. No MSCs were detected in hydrogel injected without MSCs.

Discussion

In this study, we examined the efficacy of an injectable therapy for intervertebral disc degeneration that combines a triple interpenetrating network hydrogel implant and MSCs. This therapeutic strategy is specifically designed to target patients who exhibit chronic low-back pain associated with moderate-severity degeneration, and who are not good candidates for surgical intervention and for whom conservative therapies have failed. To this end, and to maximize the clinical relevance of results, we used a large animal model that we previously optimized to mimic degenerative changes consistent with moderate-severity disc degeneration, including reduction in disc height, altered disc cellularity and extracellular matrix, and local inflammation in the NP and AF.[21,22] Importantly, and consistent with our previously published findings, injected hydrogel remained predominantly localized to the central NP region 2 weeks after delivery and for the combined treatment group, MSCs were distributed throughout the hydrogel.

MSC-based disc therapies have been explored extensively in recent years using a range of preclinical large animal models with mixed results.[26–32] Hiyama *et al.* reported that MSC injections were able to arrest progressive disc height decline in a canine disc degeneration model.[28] Two recent studies examined effects of MSC injections in a sheep AF injury-induced disc degeneration model and reported significant improvements in disc height at time points ranging from 14 weeks to 6 months posttreatment compared to phosphate-buffered saline injection alone.[27,31] In contrast, Acosta *et al.* reported minimal regenerative effects of MSCs injected in a fibrin carrier to degenerated porcine discs 3–12 months after treatment.[26] Similarly, Omlor *et al.* reported no significant improvement in disc height 1 or 12 weeks following intradiscal delivery of MSCs in a fibrin carrier to degenerate porcine discs.[30] Acute improvements in disc histological condition were reported, but these were not sustained after 12 weeks. In dogs with spontaneous and symptomatic disc degeneration, Steffen *et al.* reported negligible therapeutic benefit of MSC injections, and by some outcome measures, treatment exacerbated degeneration after 12 months.[32] Similar mixed findings have been reported in human clinical trials,[9] preventing widespread clinical adoption of such therapies, and reflecting the need for ongoing efforts to enhance the *in vivo* survival and performance of MSCs in the degenerate disc microenvironment.

Hydrogel carriers that mimic native NP tissue biomechanical properties have the potential to both acutely stabilize disc structure and mechanical function, and enhance cell retention, survival, and performance. A wide range of different hydrogel formulations has been explored,[10] and *ex vivo* and *in vivo* animal studies have demonstrated the potential of these materials to stabilize or improve degenerate or nucleotomized disc biomechanical properties[19,33–37] and/or support delivery of therapeutic cells.[20,38–43] The triple interpenetrating network hydrogel evaluated in this study exhibits the essential characteristics described above, highlighting its potential as both an effective NP structural implant and MSC delivery vehicle.[18,20] Our results showed that treatment of moderately degenerate discs with both hydrogel alone and hydrogel + MSCs resulted in improvements in disc height; however, the greatest and most consistent improvement was found for discs that received the combined treatment. Change in disc height is a key metric used clinically to assess progression of disc degeneration and response to treatment.[44,45] The reasons for this are twofold: first, a reduction in disc height may result in nerve impingement and foraminal stenosis, and thus directly correlates with the presence and severity of symptoms; second, disc height changes can be readily assessed using standard

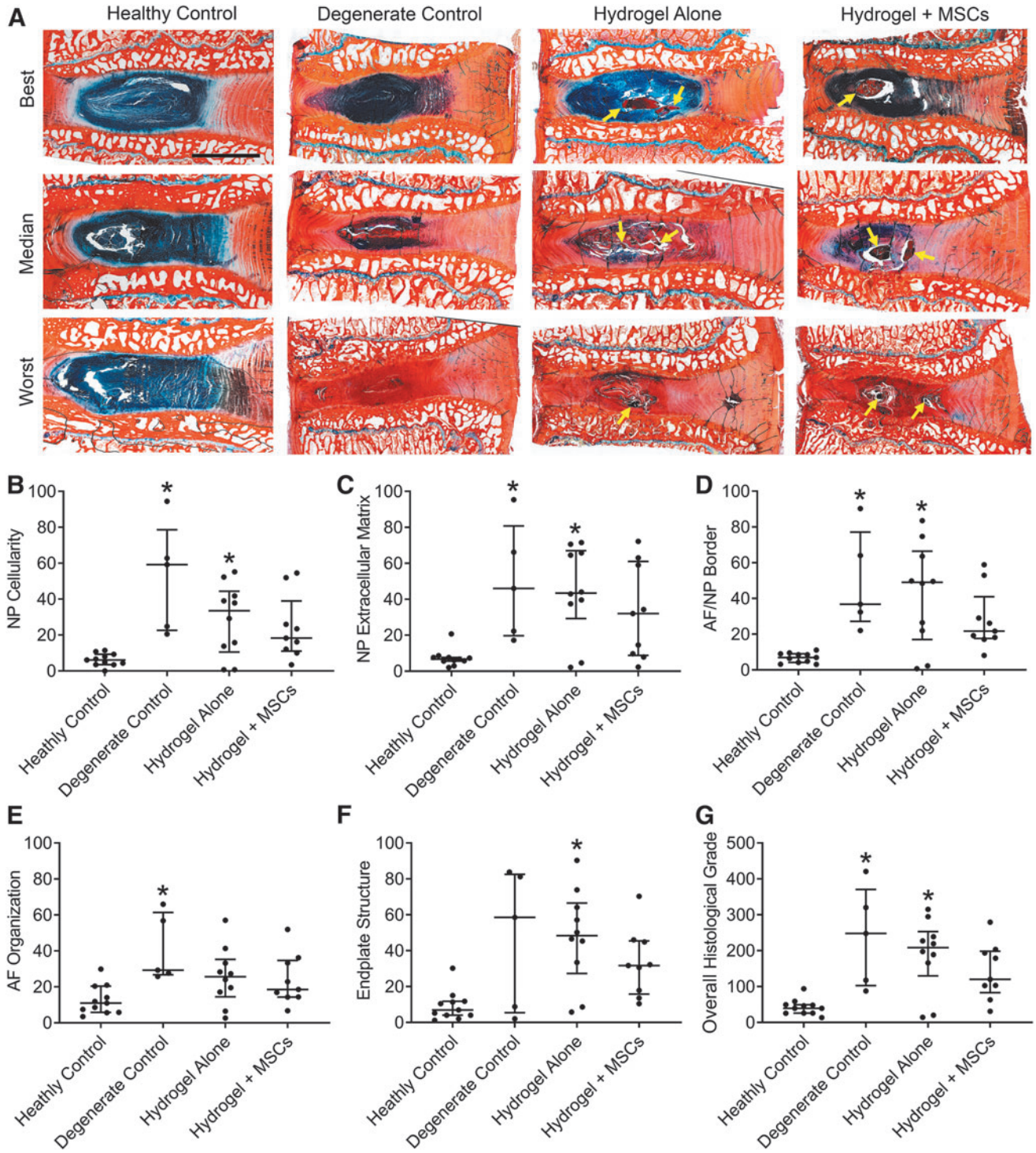

FIG. 5. **(A)** Representative histological sections illustrating best, median, and worst discs from each study group. Alcian blue (glycosaminoglycans) and picrosirius red (collagen) double-stained, mid-sagittal sections; arrows indicate locations of hydrogel; Scale = 5 mm. **(B–G)** Semiquantitative histological grading results for NP cellularity, NP extracellular matrix, AF/NP border, AF organization, endplate structure, and overall histological grade. $*p < 0.05$ versus healthy control; Kruskal-Wallis tests with *posthoc* Dunn's tests; data presented as median and interquartile range. AF, annulus fibrosus. Color images are available online.

diagnostic imaging techniques such as MRI and plain radiographs. The disc height improvements we observed in this study were complemented by histological findings, where improvements in individual grading parameters and overall histological grade were greatest for discs treated with both hydrogel and MSCs. These results suggest a therapeutic benefit of MSCs at this early, 2-week time point, and are encouraging in light of the well-documented challenges of disc regeneration using exogenous stem cells. Inflammation, low oxygen, acidity, and poor nutrient

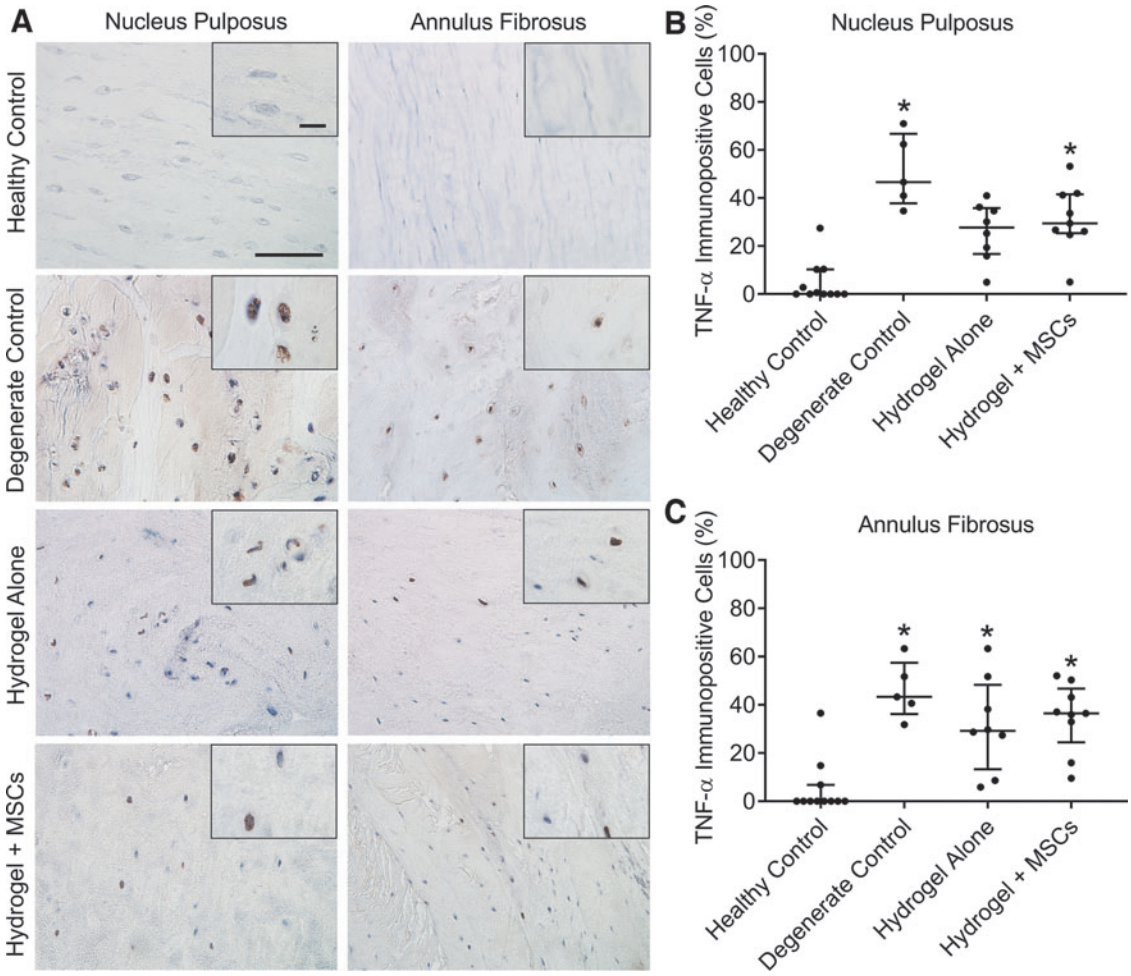

FIG. 6. **(A)** Representative immunohistochemical staining for TNF-α in the NP and AF for each study group. Scale = 100 μm (*inset* 20 μm). **(B, C)** Quantification of the number of cells immunopositive for TNF-α in the NP and AF, expressed as a percentage of total cells. $*p < 0.05$ versus healthy control; Kruskal-Wallis tests with *posthoc* Dunn's tests; data presented as median and interquartile range. TNF, tumor necrosis factor. Color images are available online.

availability have all been established as impediments to the survival and function of MSCs upon *in vivo* delivery to the degenerate NP microenvironment.[46–48] In addition to the use of an appropriate hydrogel carrier, several strategies have been proposed to enhance the *in vivo* performance of MSCs in the disc, including hypoxic preconditioning before delivery[47,49] and co-delivery of drugs to neutralize local inflammation.[50–53] While we were able to confirm the presence of MSCs within the hydrogel 2 weeks after delivery, we did not examine survival or whether these cells had adopted phenotypic characteristics conducive to tissue regeneration. This is a limitation of this study, as establishing mechanism of action is important for ensuring safety and successful future clinical translation, and will be investigated in the future. Potential mechanisms of MSC-based regeneration in the disc may include direct

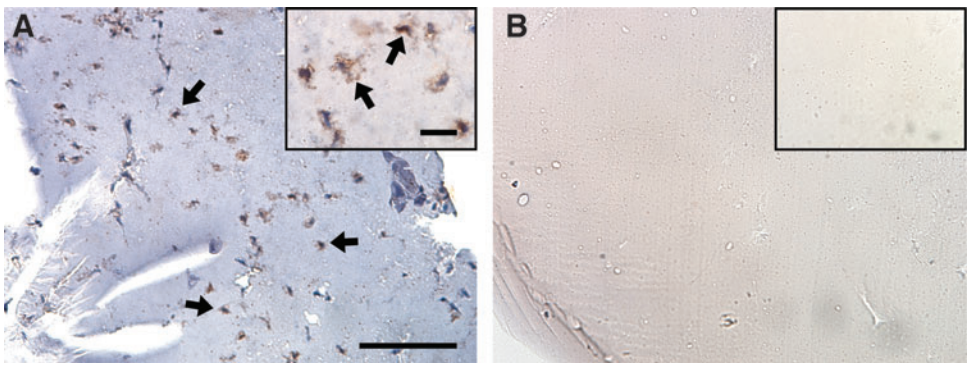

FIG. 7. Representative immunohistochemical staining of green fluorescent protein-positive MSCs in discs treated with **(A)** combined hydrogel + MSCs (*arrows* = examples) and **(B)** hydrogel alone. Scale = 100 μm (*inset* 20 μm). MSC, mesenchymal stem cell. Color images are available online.

reconstitution of native NP extracellular matrix, or paracrine signaling to endogenous cells to suppress inflammation and induce a more anabolic phenotype.[12,13,54,55]

Inflammation is not only an impediment to cell-based disc regeneration but also accelerates the degenerative cascade by driving extracellular matrix catabolism.[7] Given the established anti-inflammatory properties of MSCs, we expected that we would observe the greatest reduction in inflammation for the combined hydrogel + MSC treatment group; interestingly, however, the greatest reduction was found for discs treated with hydrogel alone. One possible explanation for these findings is that the hydrogel normalizes the local micromechanical environment for endogenous cells. Abnormal loading has been shown to upregulate inflammatory gene expression in disc cells in a range of *in vivo* and *ex vivo* model systems.[56–58] An alternative explanation is that the constituents of the hydrogel themselves impart anti-inflammatory effects. For example, chitosan, a polysaccharide with a molecular structure similar to glycosaminoglycans, has established anti-inflammatory properties, including the ability to suppress TNF-α expression.[59,60]

Interestingly, while we observed improvements in disc height and histological grade, no such improvements were found for MRI grade. It is possible that moderate improvements in disc condition at this early, 2-week time point are below the detectable limit of semiquantitative Pfirrmann grading. Alternatively, the unknown magnetic resonance properties of the hydrogel could have confounded MRI signal intensity in the NP.

There were some additional important limitations to this study. First, in a small subset of discs, we observed large endplate disruptions on imaging and histology. Similar phenomena were reported in a previous study in goats following injection of stromal vascular fraction, with and without ChABC to induce degeneration.[61] The cause of these endplate disruptions has not been determined and will be the subject of ongoing investigations, including whether they are model or species specific. An additional limitation was the fact that we did not assess potential adjacent level effects of degeneration due to biomechanical and biological crosstalk between adjacent discs. We did not assess effects of treatment of disc biomechanical properties, nor did we include pain as an outcome measure in this study. Clinically relevant changes to the cartilaginous endplates such as decreased permeability,[62,63] which my impact the supply of nutrients to therapeutic cells, may not be effectively recapitulated in this animal model. Finally, in this study, we examined therapeutic efficacy at an acute, 2-week time point. In the future, it will be important to confirm whether these encouraging findings are sustained or enhanced at longer time points.

Conclusions

In this study, we examined the efficacy of combined hydrogel and MSC injections for treatment of moderate-severity disc degeneration in a goat model. Positive effects of treatment on disc height, condition, and inflammation were observed 2 weeks after administration. In general, combined treatment with hydrogel and MSCs elicited a greater therapeutic effect, with the exception of inflammation, which responded more favorably to hydrogel alone. These encouraging findings motivate further, longer term studies of therapeutic efficacy in this large animal model.

Authors' Contributions

C.Z. performed experiments, contributed to conceptual design, and drafted the article; S.E.G. performed experiments and contributed to conceptual design; T.P.S. performed surgeries, supervised animal care, and contributed to conceptual design; S.B. contributed to animal care and performed *in vivo* experiments; D.M.E., G.R.D., and R.L.M. contributed to conceptual design; W.C. optimized and fabricated the hydrogel; N.R.M. performed surgeries and contributed to conceptual design; and L.J.S. contributed to conceptual design and drafted the article.

Acknowledgments

The authors would also like to acknowledge the veterinary staff at New Bolton Center, University of Pennsylvania School of Veterinary Medicine for assistance with animal care throughout the study.

Disclosure Statement

No competing financial interests exist.

Funding Information

This work was supported by the Department of Veterans Affairs (RR&D I01RX001321) and the Catherine D. Sharpe Foundation. Core equipment used in this study was provided by the Penn Center for Musculoskeletal Disorders (National Institutes of Health P30 AR069619).

Supplementary Material

Supplementary Figure S1

References

1. Global Burden of Disease Study Collaborators. Global, regional, and national incidence, prevalence, and years lived with disability for 301 acute and chronic diseases and injuries in 188 countries, 1990–2013: a systematic analysis for the Global Burden of Disease Study 2013. Lancet **386,** 743, 2015.
2. Dieleman, J.L., Baral, R., Birger, M., *et al.* US spending on personal health care and public health, 1996–2013. JAMA **316,** 2627, 2016.
3. Freemont, A.J. The cellular pathobiology of the degenerate intervertebral disc and discogenic back pain. Rheumatology (Oxford) **48,** 5, 2009.
4. Raj, P.P. Intervertebral disc: anatomy-physiology-pathophysiology-treatment. Pain Pract **8,** 18, 2008.
5. Hart, L.G., Deyo, R.A., and Cherkin, D.C. Physician office visits for low back pain. Frequency, clinical evaluation, and treatment patterns from a U.S. national survey. Spine (Phila Pa 1976) **20,** 11, 1995.
6. Smith, L.J., Nerurkar, N.L., Choi, K.S., Harfe, B.D., and Elliott, D.M. Degeneration and regeneration of the intervertebral disc: lessons from development. Dis Model Mech **4,** 31, 2011.
7. Le Maitre, C.L., Pockert, A., Buttlet, D.J., Freemont, A.J., and Hoyland, J.A. Matrix synthesis and degradation in human intervertebral disc degeneration. Biochem Soc Trans **35,** 652, 2007.
8. Urban, J.P., and Roberts, S. Degeneration of the intervertebral disc. Arthritis Res Ther **5,** 120, 2003.

9. Smith, L.J., Silverman, L., Sakai, D., *et al.* Advancing cell therapies for intervertebral disc regeneration from the lab to the clinic: recommendations of the ORS spine section. JOR Spine **1,** e1036, 2018.
10. Bowles, R.D., and Setton, L.A. Biomaterials for intervertebral disc regeneration and repair. Biomaterials **129,** 54, 2017.
11. Vadala, G., Russo, F., Ambrosio, L., Loppini, M., and Denaro, V. Stem cells sources for intervertebral disc regeneration. World J Stem Cells **8,** 185, 2016.
12. Risbud, M.V., Albert, T.J., Guttapalli, A., *et al.* Differentiation of mesenchymal stem cells towards a nucleus pulposus-like phenotype in vitro: implications for cell-based transplantation therapy. Spine (Phila Pa 1976) **29,** 2627, 2004.
13. Stoyanov, J.V., Gantenbein-Ritter, B., Bertolo, A., *et al.* Role of hypoxia and growth and differentiation factor-5 on differentiation of human mesenchymal stem cells towards intervertebral nucleus pulposus-like cells. Eur Cell Mater **21,** 533, 2011.
14. Barry, F.P., and Murphy, J.M. Mesenchymal stem cells: clinical applications and biological characterization. Int J Biochem Cell Biol **36,** 568, 2004.
15. Buckley, C.T., Hoyland, J.A., Fujii, K., Pandit, A., Iatridis, J.C., and Grad, S. Critical aspects and challenges for intervertebral disc repair and regeneration-harnessing advances in tissue engineering. JOR Spine **1,** e1029, 2018.
16. Weng, L., Chen, X., and Chen, W. Rheological characterization of in situ crosslinkable hydrogels formulated from oxidized dextran and *N*-carboxyethyl chitosan. Biomacromolecules **8,** 1109, 2007.
17. Zhang, H., Qadeer, A., Mynarcik, D., and Chen, W. Delivery of rosiglitazone from an injectable triple interpenetrating network hydrogel composed of naturally derived materials. Biomaterials **32,** 890, 2011.
18. Gullbrand, S.E., Schaer, T.P., Agarwal, P., *et al.* Translation of an injectable triple-interpenetrating-network hydrogel for intervertebral disc regeneration in a goat model. Acta Biomater **60,** 201, 2017.
19. Showalter, B.L., Elliott, D.M., Chen, W., and Malhotra, N.R. Evaluation of an in situ gelable and injectable hydrogel treatment to preserve human disc mechanical function undergoing physiologic cyclic loading followed by hydrated recovery. J Biomech Eng **137,** 081008, 2015.
20. Smith, L.J., Gorth, D.J., Showalter, B.L., *et al.* In vitro characterization of a stem-cell-seeded triple-interpenetrating-network hydrogel for functional regeneration of the nucleus pulposus. Tissue Eng Part A **20,** 1841, 2014.
21. Gullbrand, S.E., Malhotra, N.R., Schaer, T.P., *et al.* A large animal model that recapitulates the spectrum of human intervertebral disc degeneration. Osteoarthritis Cartilage **25,** 146, 2017.
22. Zhang, C., Gullbrand, S.E., and Schaer, T.P. Inflammatory cytokine and catabolic enzyme expression in a goat model of intervertebral disc degeneration. J Orthop Res [Epub ahead of print]; DOI: 10.1002/jor.24639, 2020.
23. Kilkenny, C., Browne, W., Cuthill, I.C., Emerson, M., Altman, D.G., and NC3Rs Reporting Guidelines Working Group. Animal research: reporting in vivo experiments: the ARRIVE guidelines. Br J Pharmacol **160,** 1577, 2010.
24. Martin, J.T., Collins, C.M., Ikuta, K., *et al.* Population average T2 MRI maps reveal quantitative regional transformations in the degenerating rabbit intervertebral disc that vary by lumbar level. J Orthop Res **33,** 140, 2015.
25. Masuda, K., Aota, Y., Muehleman, C., *et al.* A novel rabbit model of mild, reproducible disc degeneration by an anulus needle puncture: correlation between the degree of disc injury and radiological and histological appearances of disc degeneration. Spine **30,** 5, 2005.
26. Acosta, F.L., Jr., Metz, L., Adkisson, H.D., *et al.* Porcine intervertebral disc repair using allogeneic juvenile articular chondrocytes or mesenchymal stem cells. Tissue Eng Part A **17,** 3045, 2011.
27. Freeman, B.J., Kuliwaba, J.S., Jones, C.F., *et al.* Allogeneic mesenchymal precursor cells promote healing in posterolateral annular lesions and improve indices of lumbar intervertebral disc degeneration in an ovine model. Spine **41,** 1331, 2016.
28. Hiyama, A., Mochida, J., Iwashina, T, *et al.* Transplantation of mesenchymal stem cells in a canine disc degeneration model. J Orthop Res **26,** 589, 2008.
29. Melrose, J. Strategies in regenerative medicine for intervertebral disc repair using mesenchymal stem cells and bioscaffolds. Regen Med **11,** 705, 2016.
30. Omlor, G.W., Lorenz, S., Nerlich, A.G., Guehring, T., and Richter, W. Disc cell therapy with bone-marrow-derived autologous mesenchymal stromal cells in a large porcine disc degeneration model. Eur Spine J **27,** 2639, 2018.
31. Shu, C.C., Dart, A., Bell, R., *et al.* Efficacy of administered mesenchymal stem cells in the initiation and co-ordination of repair processes by resident disc cells in an ovine (Ovis aries) large destabilizing lesion model of experimental disc degeneration. JOR Spine **1,** e1037, 2018.
32. Steffen, F., Smolders, L.A., Roentgen, A.M., Bertolo, A., and Stoyanov, J. Bone marrow-derived mesenchymal stem cells as autologous therapy in dogs with naturally occurring intervertebral disc disease: feasibility, safety, and preliminary results. Tissue Eng Part C Methods **23,** 643, 2017.
33. Leckie, A.E., Akens, M.K., Woodhouse, K.A., Yee, A.J., and Whyne, C.M. Evaluation of thiol-modified hyaluronan and elastin-like polypeptide composite augmentation in early-stage disc degeneration: comparing 2 minimally invasive techniques. Spine **37,** E1296, 2012.
34. Malhotra, N.R., Han, W.M., Beckstein, J., Cloyd, J., Chen, W., and Elliott, D.M. An injectable nucleus pulposus implant restores compressive range of motion in the ovine disc. Spine **37,** E1099, 2012.
35. Sivan, S.S., Roberts, S., Urban, J.P., *et al.* Injectable hydrogels with high fixed charge density and swelling pressure for nucleus pulposus repair: biomimetic glycosaminoglycan analogues. Acta Biomater **10,** 1124, 2014.
36. Thomas, J.D., Fussell, G., Sarkar, S., Lowman, A.M., and Marcolongo, M. Synthesis and recovery characteristics of branched and grafted PNIPAAm-PEG hydrogels for the development of an injectable load-bearing nucleus pulposus replacement. Acta Biomater **6,** 1319, 2010.
37. Balkovec, C., Vernengo, A.J., and McGill, S.M. Disc height loss and restoration via injectable hydrogel influences adjacent segment mechanics in-vitro. Clin Biomech (Bristol, Avon) **36,** 1, 2016.
38. Revell, P.A., Damien, E., Di Silvio, L., Gurav, N., Longinotti, C., and Ambrosio, L. Tissue engineered intervertebral disc repair in the pig using injectable polymers. J Mater Sci Mater Med **18,** 303, 2007.
39. Hu, J., Chen, B., Guo, F., *et al.* Injectable silk fibroin/polyurethane composite hydrogel for nucleus pulposus replacement. J Mater Sci Mater Med **23,** 711, 2012.
40. Varma, D.M., DiNicolas, M.S., and Nicoll, S.B. Injectable, redox-polymerized carboxymethylcellulose hydrogels promote nucleus pulposus-like extracellular matrix elaboration

by human MSCs in a cell density-dependent manner. J Biomater Appl **33,** 576, 2018.
41. Thorpe, A.A., Dougill, G., Vickers, L., *et al.* Thermally triggered hydrogel injection into bovine intervertebral disc tissue explants induces differentiation of mesenchymal stem cells and restores mechanical function. Acta Biomater **54,** 212, 2017.
42. Nair, M.B., Baranwal, G., Vijayan, P., Keyan, K.S., and Jayakumar, R. Composite hydrogel of chitosan-poly(hydroxybutyrate-co-valerate) with chondroitin sulfate nanoparticles for nucleus pulposus tissue engineering. Colloids Surf B Biointerfaces **136,** 84, 2015.
43. Frith, J.E., Cameron, A.R., Menzies, D.J., *et al.* An injectable hydrogel incorporating mesenchymal precursor cells and pentosan polysulphate for intervertebral disc regeneration. Biomaterials **34,** 9430, 2013.
44. Thompson, J.P., Pearce, R.H., Schechter, M.T., Adams, M.E., Tsang, I.K., and Bishop, P.B. Preliminary evaluation of a scheme for grading the gross morphology of the human intervertebral disc. Spine (Phila Pa 1976) **15,** 411, 1990.
45. Pfirrmann, C.W., Metzdorf, A., Zanetti, M., Hodler, J., and Boos, N. Magnetic resonance classification of lumbar intervertebral disc degeneration. Spine (Phila Pa 1976) **26,** 1873, 2001.
46. Krock, E., Rosenzweig, D.H., and Haglund, L. The inflammatory milieu of the degenerate disc: is mesenchymal stem cell-based therapy for intervertebral disc repair a feasible approach? Curr Stem Cell Res Ther **10,** 317, 2015.
47. Peck, S.H., Bendigo, J.R., Tobias, J.W., *et al.* Hypoxic preconditioning enhances bone marrow-derived mesenchymal stem cell survival in a low oxygen and nutrient-limited 3D microenvironment. Cartilage [Epub ahead of print]; DOI: 10.1177/1947603519841675, 2019.
48. Naqvi, S.M., and Buckley, C.T. Bone marrow stem cells in response to intervertebral disc-like matrix acidity and oxygen concentration: implications for cell-based regenerative therapy. Spine (Phila Pa 1976) **41,** 743, 2016.
49. Chiang, E.R., Ma, H.L., Wang, J.P., *et al.* Use of allogeneic hypoxic mesenchymal stem cells for treating disc degeneration in rabbits. J Orthop Res **37,** 1440, 2019.
50. Gorth, D.J., Martin, J.T., Dodge, G.R., *et al.* In vivo retention and bioactivity of IL-1ra microspheres in the rat intervertebral disc: a preliminary investigation. J Exp Orthop **1,** 15, 2014.
51. Gorth, D.J., Mauck, R.L., Chiaro, J.A., *et al.* IL-1ra delivered from poly(lactic-co-glycolic acid) microspheres attenuates IL-1 beta-mediated degradation of nucleus pulposus in vitro. Arthritis Res Ther **14,** R179, 2012.
52. Le Maitre, C.L., Hoyland, J.A., and Freemont, A.J. Interleukin-1 receptor antagonist delivered directly and by gene therapy inhibits matrix degradation in the intact degenerate human intervertebral disc: an in situ zymographic and gene therapy study. Arthritis Res Ther **9,** R83, 2007.
53. Walter, B.A., Purmessur, D., Likhitpanichkul, M., *et al.* Inflammatory kinetics and efficacy of anti-inflammatory treatments on human nucleus pulposus cells. Spine (Phila Pa 1976) **40,** 955, 2015.
54. Hingert, D., Nawilaijaroen, P., Aldridge, J., Baranto, A., and Brisby, H. Investigation of the effect of secreted factors from mesenchymal stem cells on disc cells from degenerated discs. Cells Tissues Organs **208,** 76, 2020.
55. Teixeira, G.Q., Pereira, C.L., Ferreira, J.R., *et al.* Immunomodulation of human mesenchymal stem/stromal cells in intervertebral disc degeneration: insights from a proinflammatory/degenerative ex vivo model. Spine (Phila Pa 1976) **43,** E673, 2018.
56. Paul, C.P., Schoorl, T., Zuiderbaan, H.A., *et al.* Dynamic and static overloading induce early degenerative processes in caprine lumbar intervertebral discs. PLoS One **8,** e62411, 2013.
57. Gawri, R., Rosenzweig, D.H., Krock, E., *et al.* High mechanical strain of primary intervertebral disc cells promotes secretion of inflammatory factors associated with disc degeneration and pain. Arthritis Res Ther **16,** R21, 2014.
58. Yurube, T., Takada, T., Suzuki, T., *et al.* Rat tail static compression model mimics extracellular matrix metabolic imbalances of matrix metalloproteinases, aggrecanases, and tissue inhibitors of metalloproteinases in intervertebral disc degeneration. Arthritis Res Ther **14,** R51, 2012.
59. Chung, M.J., Park, J.K., and Il Park, Y. Anti-inflammatory effects of low-molecular weight chitosan oligosaccharides in IgE-antigen complex-stimulated RBL-2H3 cells and asthma model mice. Int Immunopharmacol **12,** 453, 2012.
60. Kim, S. Competitive biological activities of chitosan and its derivatives: antimicrobial, antioxidant, anticancer, and anti-inflammatory activities. Int J Polym Sci **2018,** 1, 2018.
61. Detiger, S.E., Helder, M.N., Smit, T.H., and Hoogendoorn, R.J. Adverse effects of stromal vascular fraction during regenerative treatment of the intervertebral disc: observations in a goat model. Eur Spine J **24,** 1992, 2015.
62. DeLucca, J.F., Cortes, D.H., Jacobs, N.T., Vresilovic, E.J., Duncan, R.L., and Elliott, D.M. Human cartilage endplate permeability varies with degeneration and intervertebral disc site. J Biomech **49,** 550, 2016.
63. Wong, J., Sampson, S.L., Bell-Briones, H., *et al.* Nutrient supply and nucleus pulposus cell function: effects of the transport properties of the cartilage endplate and potential implications for intradiscal biologic therapy. Osteoarthritis Cartilage **27,** 956, 2019.

Address correspondence to:
Lachlan J. Smith, PhD
Department of Neurosurgery
Perelman School of Medicine
University of Pennsylvania
3450 Hamilton Walk
Philadelphia, PA 19104
USA

E-mail: lachlans@pennmedicine.upenn.edu

Neil R. Malhotra, MD
Department of Neurosurgery
Perelman School of Medicine
University of Pennsylvania
3450 Hamilton Walk
Philadelphia, PA 19104
USA

E-mail: nrm@uphs.upenn.edu

Received: April 22, 2020
Accepted: June 1, 2020
Online Publication Date: August 10, 2020